The Journal of CPRI,
Vol. 9, No. 4, December 2013 pp. 557-564

Design and Performance Evaluation of Standalone Solar-PV System Using Interval FLC Based MPPT Controller

Neha Adhikari*, Bhim Singh** and Vyas A L***

This paper deals with the design, modeling and performance evaluation of standalone solar-PV (Photo-Voltaic) system using interval type FLC (Fuzzy Logic Controller) based MPPT (Maximum Power Point Tracking) controller. The proposed system is designed for a 5 kW solar-PV generating system. The system consists of a solar-PV array connected with the single phase VSI (Voltage Source Inverter) through a MPPT controller and an LCL filter is used to feed the power to the consumer loads. The design procedure and modeling of the system components and controller is presented in detail. The performance of the system is evaluated in steady and dynamic system conditions to validate its design and model. The voltage controller is designed to maintain the dc link voltage and performing under varying input voltages. The output voltage and current regulator is designed to maintain the power quality under varying consumer loads and results are presented for THD (Total Harmonic Distortion) which are found under the limits of 5%.

Keywords: *Solar Photovoltaic, MPPT control, FLC controllers, Isolated Cuk Converter*

1.0 INTRODUCTION

Solar photovoltaic (SPV) systems in standalone applications are useful in rural areas as it is easily available source. However, it requires a controller to extract maximum power from the solar-PV array and maintain the output power quality under load variations. Power converters are used to convert the dc power from solar panels to ac power, which can be connected either to existing electrical grid system or it may used in standalone systems. Different types of MPPT control algorithms and power converter topologies are presented in the literature to study the system performance [1-3]. The solar systems can be categorized mainly into two categories as single stage and dual stage systems. The single stage system consists of only one stage of power conversion, and dc-ac converters are used in such systems. The single stage system offers advantage of reduced system components however the control complexity in such systems is high. It requires a solar-PV array with high voltage ratings, which leads to drawbacks such as hot-spots during partial shading of the array, reduced safety and increased probability of leakage current through the parasitic capacitance between the panel and the system ground [4-5]. The dual stage system includes a dc-dc conversion as an additional stage, and this offers the comparatively simple control system and can accommodate the solar panels of lower voltages. In the proposed system, the dual stage power conversion is used. The isolated Cuk converter is used as dc-dc converter as it can be used for both step-up and step down voltages and thus can accommodate the wide range of solar-PV output voltage. The detailed design and modeling of the system is presented along with the performance of the system under steady and dynamic conditions.

*Engineering Officer Grade-3, Energy Efficiency and Renewable Energy Division, CPRI, Bangalore-560080, India. E-mail: nehaadhikari@cpri.in
**Professor, Department of Electrical Engineering, Indian Institute of Technology, Delhi, New Delhi-110016, India. E-mail: bhimsinghiitd@gmail.com
***Professor, Instrument Design and Development Centre, Indian Institute of Technology, Delhi, New Delhi-110016, India. E-mail: alvyas@iddc.iitd.ac.in

2.0 SYSTEM CONFIGURATION

Figure 1 shows the proposed system configuration. It includes a solar-PV array, an isolated Cuk converter, battery, single phase VSI (Voltage Source Inverter), MPPT controller and voltage and current regulator.

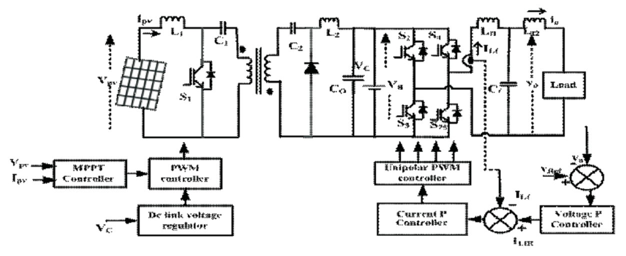

FIG. 1 SYSTEM CONFIGURATION OF DUAL STAGE SOLAR-PV SYSTEM

The Cuk converter is used to regulate the output voltage of solar-PV array through a MPPT controller and a voltage regulator of VSI is used to maintain the power quality at the consumer load end. The battery is used in the system to store the energy for feeding the average load of 2kW for 8 hours. Thus 16 numbers of batteries 24V, 40Ah are selected for the system.

3.0 CHARACTERISTICS OF SOLAR-PV ARRAY

The power output of solar-PV array is a function of operating temperature and solar radiations. The output power varies nonlinearly with the variations in the solar radiation and temperature. The characteristics of solar cell can be expressed with its diode equivalent model i.e. a current source in parallel with a diode and series and parallel resistances [6-7]. The current source represents the photo generated current. The series resistance represents the internal cell resistance. The output current of solar cell can be expressed as,

$$I_{PV} = n_P I_{pg} - n_P I_d \left(\exp^{\frac{q\left(V_{pv}\; n_S + I_{pv} R_S\; n_P\right)}{nkT}} - 1 \right) - \frac{n_P\; n_S\; V_{PV} + I_{PV} R_S}{R_{SH}} \qquad ....(1)$$

where the n_p is number of cells in parallel and n_s is the number of cells in series. The output voltage and current of solar cell is V_{pv} and I_{pv}. The photo generated current is I_{pg} and k is the Boltzmann constant, and T is the operating temperature of the cell. A set of 250 W solar panels 20 in numbers are connected in series-parallel combinations to realize a 5 kW array. Figure 2 shows the characteristics obtained from the model.

The power-voltage and voltage-current curves are calculated under various solar radiations. From the obtained characteristics it can be observed that for a specific value of solar radiation, the maximum power can be obtained by operating of specific value of voltage and current termed as MPP (Maximum Power Point). The operating point of MPP varies with the variation in solar radiations. Thus the MPPT controller is incorporated in the system to track this point.

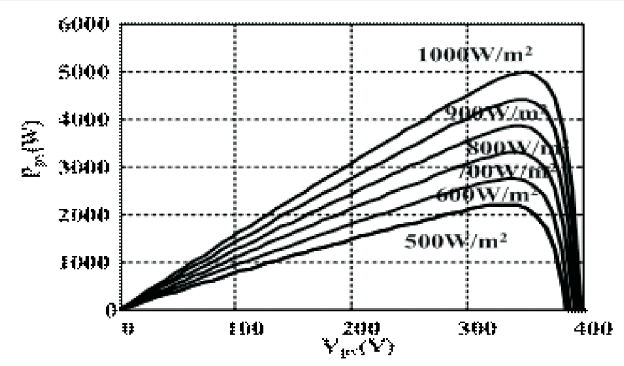

FIG. 2 POWER- VOLTAGE CHARACTERISTICS OF SOLAR-PV ARRAY

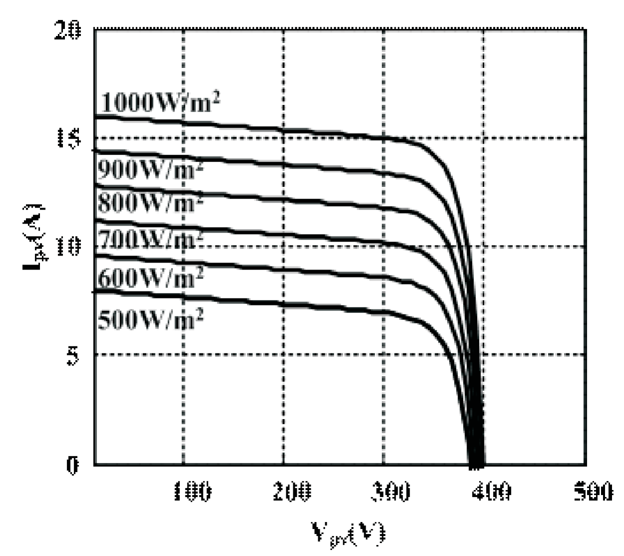

FIG. 3 CURRENT- VOLTAGE CHARACTERISTICS OF SOLAR-PV ARRAY

The value of MPP varies with the variation in solar radiations. Thus the MPPT controller is incorporated in the system to track this point.

4.0 DESIGN OF SYSTEM COMPONENTS

This section covers the detailed design of system components. The power converters used in the system include an isolated Cuk converter and a single phase VSI. The LCL filter is used for feeding the generated power to the loads. The design of the proposed system is presented as follows.

4.1 Design of Power Converters

Figure 1 shows the circuit configuration of the proposed system. An isolated Cuk converter and a single phase VSI are used in the system as power converters. The Cuk converter is a buck-boost converter i.e. it can be used for both step up and step down operation of the dc voltage. The Cuk converter combines the characteristics of boost converter i.e. lower ripples in the input current and the characteristics of buck converter i.e. lower ripples in the output current [8-10]. Another advantage of this converter is only one switching device is required. The output voltage of Cuk converter can be expressed as,

$$V_C = \frac{d_1 . n . V_{in}}{1 - d_1} \quad ....(2)$$

where the output voltage of Cuk converter is V_C. The duty ratio of the converter is d_1. The transformer turns ratio is n and input voltage to the converter is V_{in}. The turn ratio for transformer is estimated as 1:2. The value of the input inductor of the Cuk converter can be calculated considering the allowed ripple current in the input inductor and it is considered as 1A. The value of input inductor is calculated as,

$$L_1 = \frac{V_{in} d_1}{f_{s1} \Delta i_{L1}} \quad ....(3)$$

The value of input inductor is obtained as 2 mH, considering the switching frequency as 60kHz. The value of output inductor is calculated considering the allowed ripple current in the output as 1A as follows,

$$L_2 = \frac{V_o (1 - d_1)}{f_{s1} \Delta i_{L2}} \quad ....(4)$$

The value of output inductor is calculated as 2.5mH.

The input capacitor stores the energy and transfers it to the output through transformer while the switch is turned off. The value of primary and secondary capacitors can be calculated considering the allowed ripple voltage as 5V as follows,

$$C_1 = \frac{I_{in} n^2 d_1^2}{f_{s2} (1 - d_1) \Delta V_{C1}} \quad ....(5)$$

$$C_1 = \frac{I_o d_1}{f_{s1} \Delta V_{C2}} \quad ....(6)$$

The value of output primary and secondary capacitors is calculated as 100μF and 80μF. The values of these capacitors of Cuk converter are obtained considering the input voltage as 250-350V and the output voltage as 380V.

A single phase VSI is used for feeding the ac power to the consumers. The maximum power is considered as 6.25 kVA, considering 0.8 power factor. The supply voltage is 230 V, 50 Hz, thus the device ratings are obtained as 600V, 40A.

4.2 Design of LCL Filter

The LCL filters are getting attention due to their advantages of attenuating the harmonics at lower frequencies, which is a significant feature for high power applications, and also their capacity for precise control of the output current [11-13]. The selection of inductor and capacitor in the filter is a significant effect on the output power quality. For high value of capacitor, the reactive power flowing into the capacitor is high and this leads to high current drawing from inverter side filter inductor. The capacitor cannot be too small either because this increases the inductor value hence inductor is large in order to meet the desired attenuation. Considering the reactive power as

15% of the rated power, the value of capacitor can be calculated as,

$$C_f = \frac{0.15P_O}{2\pi f_{sl} v_o^2} \quad \text{....(7)}$$

The filter capacitance is calculated as 35.8μF.

The value of filter inductors is calculated considering the resonance frequency as 5 kHz as follows,

$$f_r = \frac{1}{2\pi}\sqrt{\frac{L_i + L_g}{L_i L_g C_f}} \quad \text{....(8)}$$

Considering, the inverter side inductor and supply side inductor as same value, the value of filter inductance is calculated as, 2.6 mH.

5.0 CONTROL STRATEGIES

The MPPT control and output voltage regulation are used in the system and the detailed design of the controllers is presented as follows.

5.1 MPPT Control Method

Figure 3 shows the structure of interval type FLC MPPT controller. The MPPT controller is used to track the maximum power under uncertainties of operating conditions and other conditions such as errors in sensor measurements, variation of sensor measurement with environmental conditions such as temperature, humidity etc and also aging of the plant, which can result in due to parameter variations. Since membership functions of the FLC controller are crisp, these uncertainties turn into account and errors may be included in the membership functions [14-15].

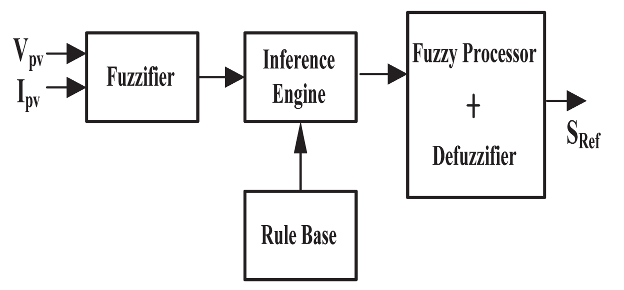

FIG. 4 MPPT CONTROL STRATEGY

The interval type FLC controller overcomes these issues by including and output processing unit in the FLC controller. The change in power and change in voltage are the input parameters to the proposed FLC controller. Figure 4 shows the membership functions of input parameters.

Fuzzification module converts the input values to the fuzzy values using the defined membership functions of the input parameters. The generated fuzzy values of input parameters are further fed to the inference engine to generate the output interval introduced fuzzy sets. Table 1 shows the rule base for the inference engine.

The seven membership functions are defined for the input parameters as NL (negative Large), NM (Negative Medium), NS (Negative Small), Z (No change), PB (Positive Big), PM (Positive medium) and PS (Positive Small).

The inference engine uses the defined rules and produces output in the form of interval fuzzy sets. Further the type reducer is used to convert these sets into fuzzy crisp output and fed it to the defuzzifier to generate the numerical output value.

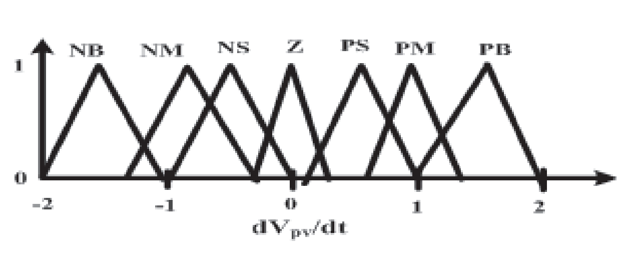

FIG. 5 MEMBERSHIP FUNCTIONS FOR CHANGE IN VOLTAGE

TABLE 1

FLC RULES FOR INFERENCE ENGINE

dP_{pv}/dt→ / dV_{pv}/dt↓	NL	NM	NS	Z	PS	PM	PB
NL	PL	NL	PL	PL	NS	PL	Z
NM	NL	NM	NM	Z	PM	PM	PL
NS	PL	NS	PL	PS	PS	PS	Z
Z	PS	Z	PS	Z	NS	Z	NS
PS	NS	PS	NS	NS	NS	NS	NL
PM	PL	PM	PS	Z	NS	NM	NL
PB	NS	PL	NS	NL	NL	NL	NL

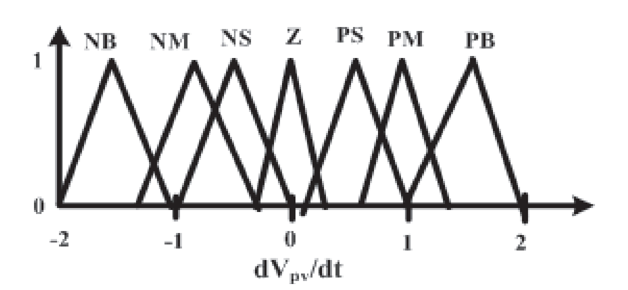

FIG. 6 MEMBERSHIP FUNCTIONS FOR CHANGE IN POWER

5.2 Voltage and Current Regulator

The power quality at the consumer end is maintained by using a P (Proportional) voltage and P current controller in cascade loop control, while the voltage control is an outer loop and current control is an inner loop control [16]. The voltage is controller and current controller are as shown in Figure 1 and the output of voltage controller is the reference current and can be presented as,

$$I_{Lref} = I_{Lref}(n-1) + k_{P1}\{v_e(n) - v_e(n-1)\} \quad ....(9)$$

The generated reference current is compared with the inductor current and fed to the P current controller, the output of current controller can be presented as,

$$V_{Sref} = I_e(n-1) + k_{P2}\{I_e(n) - I_e(n-1)\} \quad ....(10)$$

The reference voltage signal is fed to the PWM controller for the generation of switching signals for the VSI devices.

6.0 RESULTS AND DISCUSSION

The performance of the system is evaluated under steady and dynamic environment conditions as follows.

6.1 Performance of the System Under Steady State Condition

Performance of the system is analyzed under steady conditions of solar radiation and the linear load conditions as shown in Figure 5

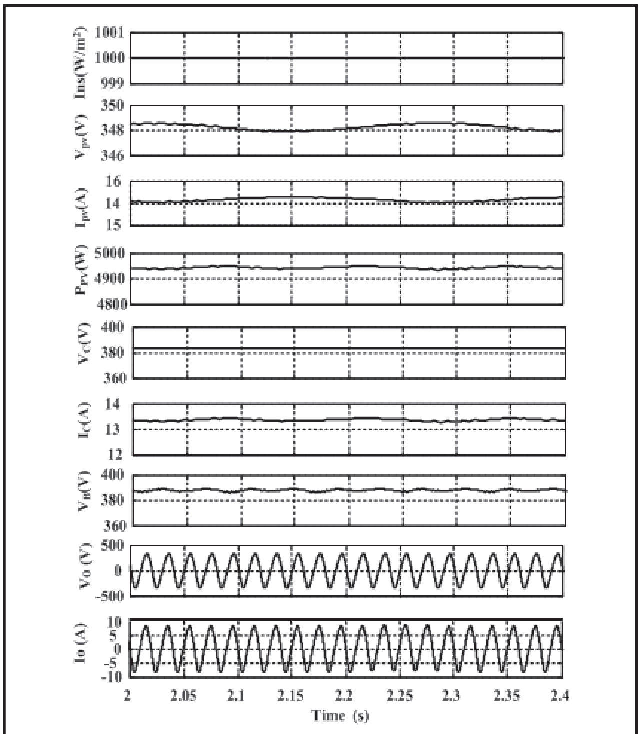

FIG. 7 PERFORMANCE OF THE SYSTEM UNDER STEADY SOLAR RADIATIONS

The solar radiations are considered as 1000W/m^2 and the consumer load is considered as 2 kW.

The output voltage (V_{pv}) and current (I_{pv}) of solar-PV array under this condition are obtained as 348V and 13.2A. The output voltage of Cuk converter is 380V. The output voltage and current at the consumer end are obtained as 230V, 8.5A. Performance of the system under steady condition is found satisfactory as the power generated by the system and the measured voltage of battery charging can be validated by the system design.

6.2 Performance of the System Under Dynamic Conditions

Performance of the system is demonstrated under dynamic conditions of solar radiations and the varying consumer loads. Figure 6 shows the performance of the system under varying solar radiations. The solar radiations are considered as varying at 2.15s and the radiations are decreased to 600W/m^2 from the rated value of 1000W/m^2.

The variation in the voltage and current output of solar-PV array can be observed due to the variation in solar radiations. The system obtained the new value of operating voltage and current. The dc link voltage regulator is maintaining the output voltage of converter at 380V in spite of variation in the input voltage. The consumer load in this case in considered as steady thus the output voltage and current are found as sinusoidal.

The performance of the designed system is also evaluated under the consumer load variation conditions as in Figure 9. The consumer load is considered to be varying at 2.15s and solar radiations are considered at 800W/m^2.

The output voltage and current of solar-PV array is observed as 332V and 12.1A, under this conditions the output voltage of dc-dc converter is same as 380V and due to variation in the consumer load the variation in the output current can be observed. The performance of output voltage and current regulator is validated as it maintains the output voltage in spite of change in the consumer loads.

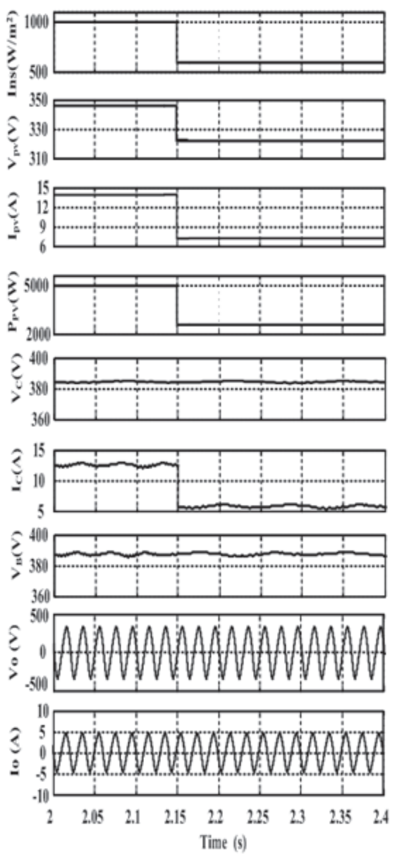

FIG. 8 PERFORMANCE OF THE SYSTEM UNDER STEADY SOLAR RADIATIONS

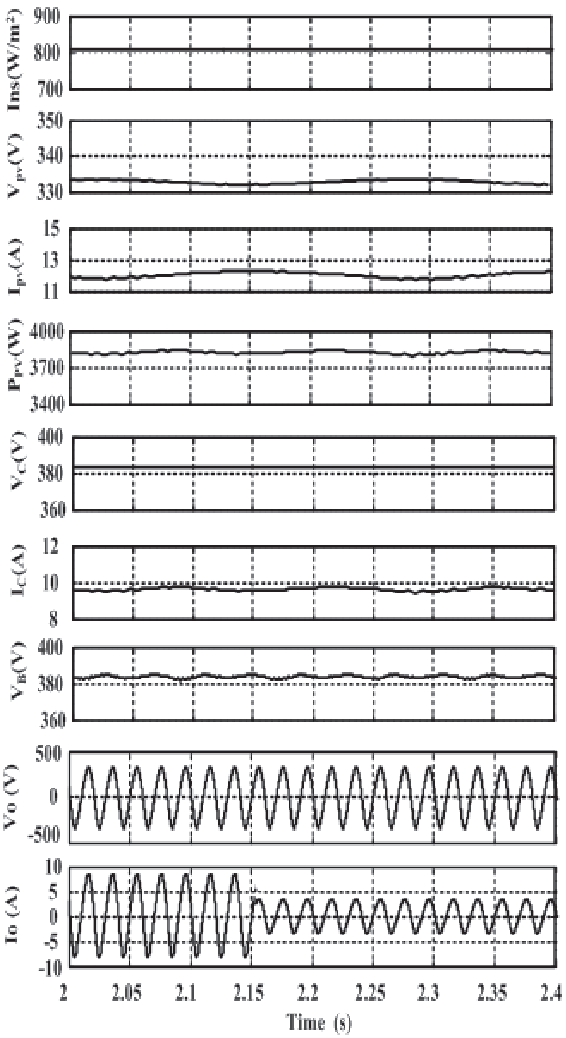

FIG. 9 PERFORMANCE OF THE SYSTEM UNDER LOAD VARIATIONS

6.3 Harmonic Spectra of Output Voltage and Current

The harmonic spectra of output voltage and current under linear consumer loads are obtained as shown in Figure 10-11 and Figure12-13. The THD (Total Harmonic Distortion) for output voltage and current respectively is obtained as 2.48% and 2.34%.

The harmonic spectra of output voltage and current under non-linear consumer loads are obtained as shown in Figure 9. The THD (Total Harmonic Distortion) for output voltage and current respectively is obtained as 2.43% and 52.65%.

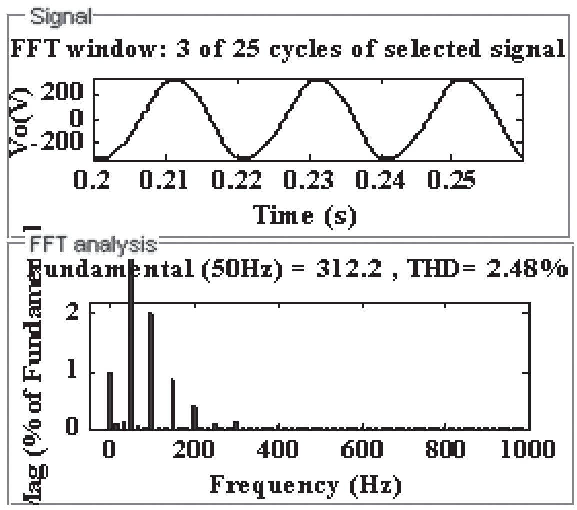

FIG. 10 HARMONIC SPECTRA OF OUTPUT VOLTAGE UNDER LINEAR LOAD

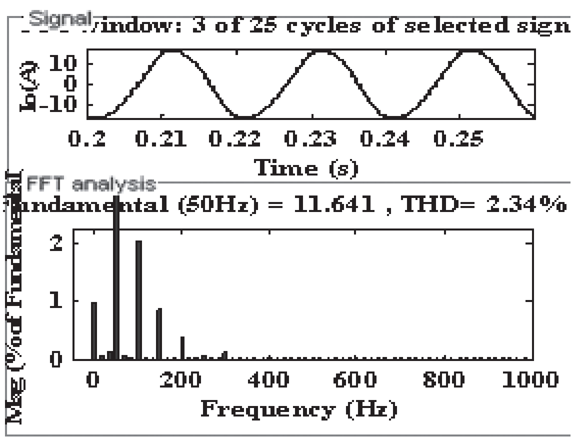

FIG. 11 HARMONIC SPECTRA OF OUTPUT CURRENT UNDER LINEAR LOAD

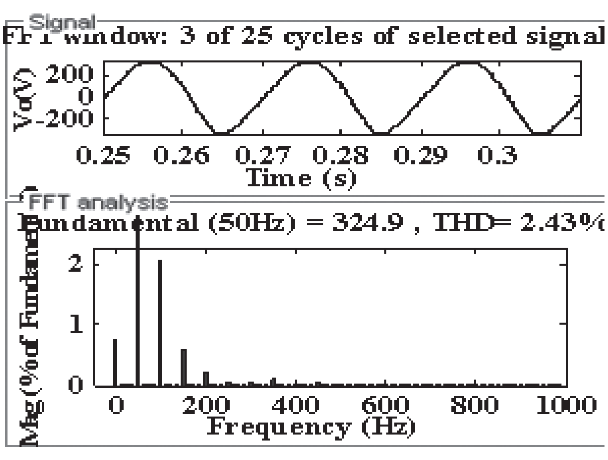

FIG. 12 HARMONIC SPECTRA OF OUTPUT VOLTAGE UNDER NONLINEAR LOAD

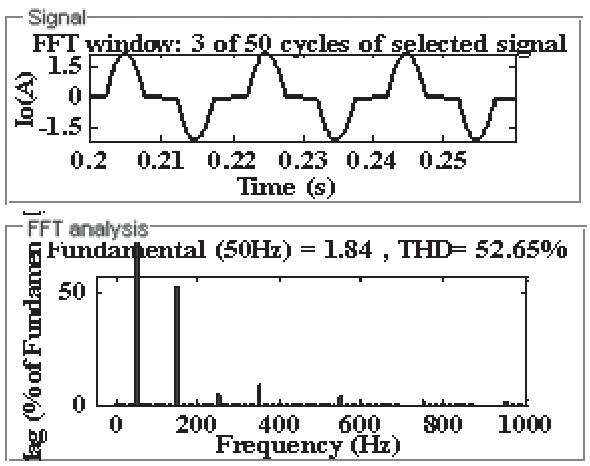

FIG. 13 HARMONIC SPECTRA OF OUTPUT CURRENT UNDER NONLINEAR LOAD

7.0 CONCLUSION

The standalone solar-PV system using an isolated Cuk converter and single phase VSI has been designed and its performance has been demonstrated in steady state and dynamic environment conditions. The detailed design procedure has been illustrated for the system and its controller. Performance of MPPT controller to track maximum power under varying solar radiations has been found satisfactorily. The response time of the controller has been observed in range of few milliseconds that is justified for solar applications as per IEC 62093 and IEC 61683. The THD for output voltage has been found under the limit of 5% as per the IEC-61000 and IEEE-519 standard. The system has been found as feasible option with low control complexity to operate under various environmental conditions.

Appendix- Solar Array- Voltage at maximum power point (v_{mp}) = 350V, Open Circuit Voltage 380V, Current at maximum power point (I_{mp}) = 13.2A, Short circuit current (I_{SC}) = 15A, Cuk Converter- Input voltage (V_{in}) = 250-350V, Primary side capacitor (C_1) = 100µF, Input Inductor (L_1) = 2 mH, Secondary side capacitor (C_1) = 80 µF , Output Inductor (L_2) = 2.5 mH, Output capacitor (C_O) = 50µF , Filter Inductor (L_f) = 2.6 mH, Filter Capacitor (C_f) = 35.8µF, Controller gains- proportional gain (k_{p1}) = 4.67, proportional gain (k_{p2}) = 1.21, Non linear load- diode bridge rectifier with R = 50Ω and C = 250µF.

REFERENCES

[1] Soeren Baekhoej Kjaer, K John and Pedersen, “A Review of Single-Phase Grid-Connected Inverters for Photovoltaic Modules,” *IEEE Trans. on Industry Applications*, vol.41 no.5, pp.1292-1306, Oct. 2005.

[2] L. Hassaine, E. Olias, J Quintero and M. Haddadi, “Digital Power Factor Control and Reactive Power Regulation for Grid-Connected Photovoltaic Inverter,” Renewable Energy, vol. 34, no.1, pp. 315-321, 2009.

[3] F. Blaabjerg, R. Teodorescu, M. Liserre and A. V. Timbus, "Overview of control and grid synchronization for distributed power generation systems," *IEEE Trans. on Industrial Electronics*, vol. 53, no.5 , pp. 1398-1409, Oct. 2006.

[4] Y. Xue, L. Chang, S. B. Kjaer, J. Bordonau and T. Shimizu, "Topologies of single-phase inverters for small distributed power generators: an overview", *IEEE Trans. Power Electron.*, vol. 19, no. 5, pp.1305 -1314, 2004.

[5] V. Timbus , M. Liserre , R. Teodorescu and F. Blaabjerg "Synchronization methods for three phase distributed power generation systems. An overview and evaluation", *Proc. IEEE PESC*, pp.2474 -2481, 2005.

[6] M. A. S. Masoum, H. Dehbonei and E. F. Fuchs. "Theoretical and Experimental Analyses of Photovoltaic Systems with Voltage- and Current-Based Maximum Power-Point Tracking", *IEEE Transactions on Energy Conversion*, vol. 17, no. 4, pp.514-522, Dec. 2002.

[7] J. A. Gow and C. D. Manning "Development of a photovoltaic array model for use in power electronics simulation studies," *IEE Proceedings on Electric Power Applications*, vol. 146, no. 2, pp. 193-200, Mar. 1999.

[8] H. Tao, A. Kotsopoulos, J. L. Duarte and M. A. M. Hendrix, "Family of multiport bidirectional DC-DC converters," *IEE Proceedings of Electric Power Applications,* vol. 153, no.1 pp. 451-458, 2006.

[9] N. Mohan, T. M. Undeland and W. P. Robbins, *‘Power Electronics: Converters, Application, and Design*,’ John Wiley & Sons, Inc., Toronto,1989.

[10] R. W. Erickson and D. Maksimovic, ‘Fundamentals of Power Electronics,’ 2nd ed., Kluwer Academic Publishers, 2001.

[11] Chen, Chien-Liang, Jih-Sheng Lai, Yu-Bin Wang, Sung-Yeul Park and H. Miwa, “Design and Control for LCL-Based Inverters with Both Grid-Tie and Standalone Parallel Operations,” in the *Proc. of IEEE Industry Applications Society Annual Meeting*, pp. 1-7, Edmonton, Canada, 5-9 Oct. 2008.

[12] F. Blaabjerg, F. Iov, R. Teodorescu and Z. Chen, "Power electronics in renewable energy systems", in the *Proc. of 12th International Power Electronics and Motion Control Conference (EPE-PEMC 2006),* pp. 1-17, Japan, August 2006.

[13] N. Pogaku, M. Prodanovic and T.C. Green, "Modeling, Analysis and Testing of Autonomous Operation of an Inverter-Based Microgrid," *IEEE Trans. on Power Electronics*, vol.22, no.2, pp.613-625, March 2007.

[14] J.M. Mendel, ‘*Rule-Based Fuzzy Logic Systems: Introduction and New Directions*,’ Prentice-Hall, Englewood Cliffs, NJ, 2001.

[15] J. M. Mendel, R. John and F. Liu, "*Interval Type-2 Fuzzy Logic Systems Made Simple*," *IEEE Trans. on Fuzzy Systems*, vol. 14, no. 6, 2006.

[16] Abdel Rahim, M. Naser and Quaicoe E. John, “Analysis and design of a multiple feedback loop control strategy for single-phase voltage-source UPS inverters,” *IEEE Trans. on Power Electronics*, vol. 11, no.4, pp. 532-541, Jul. 1996.